

## Polyether modified benzimidazole as corrosion inhibitor for copper in sodium chloride solution

Xiaoyong Xi<sup>a</sup>, Qiuli Nan<sup>b</sup>, Yuming Zhou<sup>a,b,\*</sup>, Qingzhao Yao<sup>a,\*</sup>, Li Song<sup>a</sup>, Yiyi Chen<sup>a</sup>, Shengqiu Lin<sup>a</sup>, Guiyu Guan<sup>a</sup>

<sup>a</sup>School of Chemistry and Chemical Engineering, Southeast University, Nanjing 211189, China, Tel. +86 25 52090617; emails: ymzhou@seu.edu.cn (Y. Zhou), 101006377@seu.edu.cn (Q. Yao), 2417038444@qq.com (X. Xi), 1612099899@qq.com (L. Song), cheniyi0220@126.com (Y. Chen), 1329099896@qq.com (S. Lin), 1252474476@qq.com (G. Guan)

<sup>b</sup>School of Pharmaceutical and Chemical Engineering, Cheng Xian College of Southeast University, Nanjing, Jiangsu Province 211189, China, Tel. +86 25 52090617; email: 53212651@qq.com (Q. Nan)

Received 25 March 2019; Accepted 10 December 2019

### ABSTRACT

A new kind of modified benzotriazole derivative with polyether chain o-phenylenediamine (OPD)/MPEM was synthesized as corrosion inhibition for copper in 3.5 wt.% NaCl solution. The corrosion inhibition efficiency was estimated using weight loss measurement, electrochemical methods (Tafel and EIS) and surface analysis scanning electron microscopy. Moreover, corrosion inhibition mechanism was also conducted by the electrochemical determination, the adsorption isotherm as well as the quantum chemical calculation computational methods. All measurements show that OPD/MPEM acts as an efficient corrosion inhibitor and also displays a superior ability to prevent the corrosion of copper in NaCl solution with approximately 88.0% inhibition efficiency at the low level of 60 mg L<sup>-1</sup>. Computational methods also tell that the inhibitors possess high reactivity and strong interaction on the iron surface. Furthermore, the conclusion is in good agreement with the experimental results.

*Keywords:* Copper corrosion inhibitor; Benzimidazole; Polyether; Corrosion inhibition

### 1. Introduction

Copper and its alloys have been widely used in various fields such as electronics, solar cells, structural materials, handicrafts, currency, and industrial production in the thermal cycle system due to their good thermal conductivity, superior mechanical and electric properties as well as the behavior of their passivation layer [1]. Under normal conditions, copper and its alloys are stable enough. However, they are very susceptible to undergo electrochemical corrosion under the conditions of oxidizing acid, high concentrations of Cl<sup>-</sup>, CN<sup>-</sup>, and NH<sub>4</sub><sup>+</sup> in solutions, which will shorten their service life. It is well accepted that the chloride ion has

a serious influence on copper corrosion [2,3]. Therefore, the corrosion of copper and its alloys has been widely studied in chloride media and a large number of scientists have investigated the copper dissolution mechanism in chloride solutions [4–7]. It is well known that the addition of corrosion inhibitors is the most effective and common measures in industrial applications [8]. At present, effective copper corrosion inhibitors in NaCl solutions are generally substances containing atoms like N, P, and S, such as imidazole, benzimidazole, benzotriazole, thiadiazole and their derivatives [9]. Unfortunately, these compounds are generally biologically toxic and harmful to health and the environment. Therefore,

\* Corresponding authors.

it is urgent to develop a new kind of green, efficient and harmless copper corrosion inhibitor.

As a common acid-washing corrosion inhibitor, benzimidazole (BIM) has the advantages of high efficiency, low toxicity and easy degradation [10]. Moreover, its application can reduce acid dosages and depress the metal corrosion in acid medium. Nevertheless, challenges still exist. BIM has poor solubility and is difficult to degrade. Therefore, scholars all over the world have improved the performance of benzimidazole by modifying benzimidazole derivatives. For example, Rbaa, M and co-workers have synthesized a new benzimidazoles derivative of 8-hydroxyquinoline, which exhibited a very good performance as inhibitors for mild steel corrosion in 1.0 M HCl. Their inhibitive action against the corrosion of mild steel in 1.0 M hydrochloric acid solution was investigated at different temperatures by a series of known techniques such as weight loss, polarization, and electrochemical impedance spectroscopy (EIS). However, nitrogenous compounds were still used to modify benzimidazole. Polyethylene glycol monomethyl ether (MPEG) is a green water-soluble polymer and widely used in the pharmaceutical industry and cosmetics manufacturing. As a monomer, MPEG has high water solubility and high reaction activity (affected by the polymer's structure). Meanwhile, MPEG is very cheap, easy to get and thermally stable, catering for the development of times and economy.

In this article, a new kind of modified corrosion inhibitor (OPD/MPPEM) was synthesized in acid medium, using MPEG, oxalic acid and o-phenylenediamine (OPD) under the protection of nitrogen. The weight loss, electrochemical techniques, surface morphology analysis scanning electron microscopy and energy-dispersive X-ray spectroscopy (SEM and EDX), quantum chemical calculations were applied to investigate the inhibitory performance of OPD/MPPEM. Moreover, the possible inhibition mechanism was illustrated and discussed in this study. The results presented in this study would benefit the synthesis of new efficient organic corrosion inhibitors for copper in NaCl solution. Particularly, a corrosion inhibitor for copper and its alloys protection, based on MPEG and OPD, has not been reported in the literature to date. This article aims to investigate the performance of a kind of green copolymer, OPD-MPEM, which is less toxic, has no phosphorus and low nitrogen.

## 2. Experimental

### 2.1. Experimental materials

The fine copper was used for the experiment and the total surface area of the sample was 25 cm<sup>2</sup> (50 mm × 25 mm × 2 mm), which were used for weight loss measurements.

The working electrodes were prepared by the pure copper (99.99 wt.%). The copper specimens were mechanically cut into a cylinder with a diameter of 5 mm and a height of 20 mm, embedded in polytetrafluoroethylene, and only a cylindrical surface was exposed to the air. Prior to all the experiments, the samples were abraded with a series of Emory papers (1,200; 1,500; and 2,000 grade). Then they were ultrasonically cleaned in ethanol and acetone and finally dried at the room temperature before the inhibition experiments.

MPEG (M(MPEG) = 200) is an industrial product coming from Jiang Su Haian Petrochemical Plant (Hai'an City, Jiangsu province, China) and the rest of the chemical reagents are analyzed pure. The preparation and the characterization of the target inhibitor molecules including Fourier-transform infrared spectroscopy (FT-IR) spectra and <sup>1</sup>H-NMR spectra in this study.

### 2.2. Experimental measurements

#### 2.2.1. Weight loss measurement

The copper specimens used for the weight loss experiments were rectangular with the dimensions of 50 mm × 25 mm × 2 mm, which were wiped with anhydrous ethanol. Then the cleaned specimens were wrapped in filter paper and put into the dryer for 4 h. Then they were weighed using an analytical balance of precision ±0.0001 g. After the weighing, the treated specimens were suspended in 1,000 mL of 3.5 wt.% NaCl solution with and without different concentrations of inhibitors for 72 h. The beaker was put into a water bath maintained at 318 K by using rotating-hanging film corrosion tester and the rotation speed is 50 rpm. After the experiment, the specimens were removed from the test solution, rinsed carefully with ultrapure water and acetone, dried in the air, and weighted accurately. The weight loss experiments were performed three times, and the mean weight loss was calculated.

#### 2.2.2. Electrochemical measurements

In this study, the standard three-electrode electrochemical cell was used containing the platinum foil as the counter electrode, the saturated calomel electrode (SCE) as the reference electrode, and the copper electrode as the working electrode. The electrochemical determinations in a routine three-electrode cell system were processed by the CHI660e electrochemical workstation. The corrosion media of all experiments was 3.5 wt.% NaCl solution without removing the air at 318 K and the rotation speed is 50 rpm. All the potentials were measured versus the SCE with a Luggin capillary was used as the reference electrode. The detection was carried out in the air saturated solution. The polarization curves were obtained from -250 to +250 mV (vs. open circuit potential (OCP)) with a 0.5 mV S<sup>-1</sup> scan rate, and the data were collected and analyzed by chi660e software.

The EIS measurements were performed at the steady OCP. The ac frequency range was extended from 100 kHz to 10 mHz with a 10 mV peak-to-peak sine wave, and the impedance data were analyzed and fitted by the ZSimpWin software.

#### 2.2.3. Scanning electron microscopy

Through the EDX and SEM, the main elements and surface morphology of the copper can be analyzed after immersed in 3.5 wt.% NaCl test solutions for 72 h in the presence and absence of the OPD/MPPEM.

#### 2.2.4. Molecular adsorption thermodynamics

Molecular adsorption thermodynamics studies the relationship between their concentrations in two phases when

the adsorption process of solute molecules at the two-phase interface at a certain temperature reaches equilibrium, and can generally be expressed as an adsorption isotherm curve. It is known that the basic information on the interaction between the organic inhibitor and the copper surface could be provided by the adsorption isotherm. In this study, adsorption isotherms of OPD/MPEM on copper surfaces were investigated using adsorption isotherms such as Flory–Huggins, Dhar–Flory–Huggins, Bockris–Swinkels, Freundlich, and Langmuir.

### 2.2.5. Quantum chemical calculations

Quantum chemical calculations were conducted using the DMol3 module in Materials Studio 7.0 software from Accelrys Inc., US. The geometry optimization of the organic inhibitors for the ground electronic state was performed at density functional theory level using Generalized Gradient Approximation/Becke–Lee–Yang–Parr (GGA/BLYP) method. The criteria of convergence were defined as a medium, and the orbital cut-off scheme was set as global. The quantum chemical parameters association with corrosion inhibition were calculated including the energy gap ( $\Delta E = E_{\text{LUMO}} - E_{\text{HOMO}}$ ) (HOMO – highest occupied molecular orbital and LUMO – lowest unoccupied molecular orbital), the ionization potential ( $I_p$ ), the electron affinity ( $E_A$ ), the dipole moment ( $\mu$ ), the electronegativity ( $\chi$ ), the global hardness ( $\eta$ ), and the fraction of electrons transferred ( $\Delta N$ ). Moreover, the calculation can investigate the effect of corrosion inhibitors structure and functional group for the inhibitory performance on copper surface.

### 2.3. Synthesis of benzimidazole-based phosphate-free polyether copper corrosion inhibitor (OPD/MPEM)

The synthesis of OPD/MPEM is shown in Fig. 1. An equimolar amount of (M(MPEG) = 200) and anhydrous oxalic acid were placed in a three-necked flask, and the reaction was stirred at 373 K for 6 h under  $N_2$  protection. Until the liquid in the bottle turns yellow-brown and then stir for 2 h to end the

reaction. And then the MPEM crude products were obtained. After cooling to room temperature, the crude product was dissolved in a saturated NaCl solution of equal volume with MPEG-200, and the mixture was stirred well. Subsequently, the mixture was further evaporated at 343 K under reduced pressure after being absorbed by anhydrous sodium sulfate. Afterward, the mixture was filtrate through a vacuum filter to get the yellow-brown liquid, which is the pure product MPEM. Finally, the MPEM is stored in brown bottles for use.

Then 3.24 g OPD (0.03 mol) and 30 mL ( $6 \text{ mol L}^{-1}$ ) HCl solution were added in a four-necked flask equipped with a mechanical stirrer, reflux condenser,  $N_2$  protection and constant pressure dropping funnel. The mixture was stirred at moderate speed and gradually warmed up to 373 K. Then 8.5 g MPEM (0.03 mol) was slowly and uniformly added through a constant pressure dropping funnel after the OPD was completely dissolved, and the reaction temperature was raised to 408 K. The reaction was refluxed for 7–10 h to complete the reaction to obtain a homogeneous liquid product. Afterward, the mixture was cooled to room temperature and the precipitated solid was removed by filtration. The remaining liquid was evaporated under reduced pressure at 343 K to remove the water to obtain a paste product, which was the benzimidazole-based phosphate-free polyether copper inhibitor OPD/MPEM.

## 3. Results and discussion

### 3.1. FT-IR and $^1\text{H-NMR}$ analysis of MPEG, MPEM and OPD/MPEM

The FT-IR spectra were detected on a VECTOR-22 instrument (Bruker Company, Germany) at room temperature. The samples were prepared as KBr pellet and were scanned against a blank KBr pellet background at wavenumber range of  $4,000\text{--}5,000 \text{ cm}^{-1}$  with a resolution of  $4.0 \text{ cm}^{-1}$ .

Fig. 2 shows the FT-IR spectra of MPEG, MPEM and OPD/MPEM. The band at around  $1,156 \text{ cm}^{-1}$  attributed to the characteristic absorption peak of the ether group ( $-\text{CH}_2\text{CH}_2\text{O}-$ ). The strong peak observed at  $1,770 \text{ cm}^{-1}$  in Fig. 2b is associated

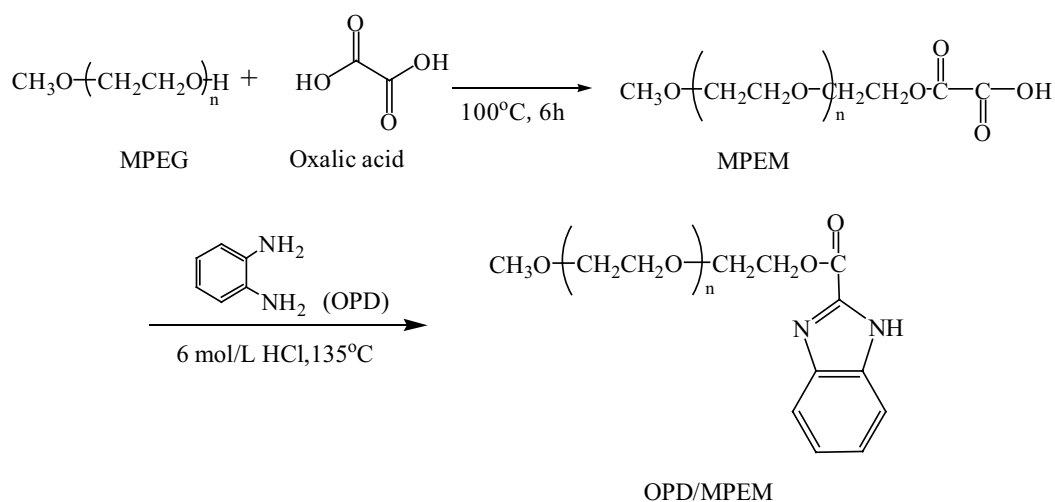


Fig. 1. Synthesis of OPD/MPEM.

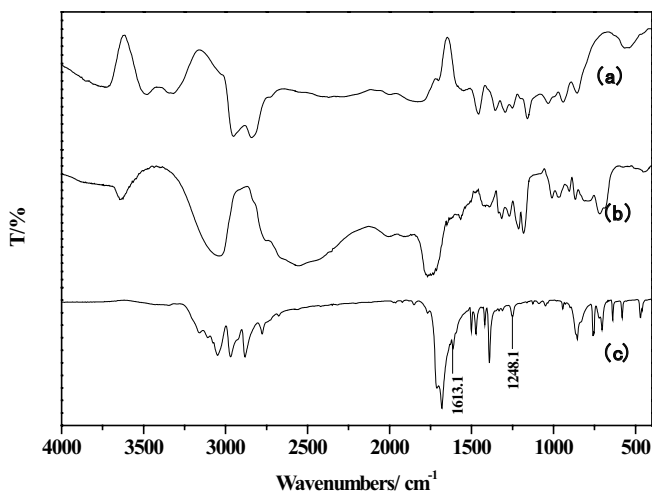


Fig. 2. FT-IR spectra of MPEG (a), MPEM (b), and OPD/MPEM (c).

with the  $\text{C}=\text{O}$  stretching vibration absorption. It reveals that MPEM has been synthesized successfully. As can be seen in Fig. 2c, the peak observed at  $3,348\text{ cm}^{-1}$  is due to the stretching vibration of  $\text{N-H}$ . The band at around  $1,680\text{ cm}^{-1}$  attributed to the  $\text{C}=\text{O}$  stretching vibration absorption. The peak at  $1,613\text{ cm}^{-1}$  assigned to the  $\text{C}=\text{N}$  of benzimidazole ring. The band at around  $1,501$  and  $1,472\text{ cm}^{-1}$  attributed to the characteristic absorption peak of  $\text{C}-\text{C}$  of benzene. All of the peaks above proved that OPD/MPEM has been synthesized successfully.

The  $^1\text{H-NMR}$  spectra were carried out on Bruker  $^1\text{H-NMR}$  analyzer (AVANCE AV-500, Bruker, Switzerland). The samples were dissolved in solvent of  $\text{DMSO-d}_6$ . Chemical shifts ( $\delta$ ) were given in parts per million using tetramethylsilane as an internal reference.

Fig. 3 shows the  $^1\text{H-NMR}$  spectra of MPEG, MPEM and OPD/MPEM.

MPEG (Fig. 3a, 400 MHz,  $\text{DMSO-d}_6$ ,  $\delta$  ppm): 2.50 (solvent residual peak of  $\text{DMSO}$ ), 3.24–3.70 ( $-\text{CH}_2\text{CH}_2\text{O}-$ , ether groups).

MPEM (Fig. 3b, 400 MHz,  $\text{DMSO-d}_6$ ,  $\delta$  ppm): 2.50 (solvent residual peak of  $\text{DMSO}$ ), 3.24–3.90 ( $-\text{CH}_2\text{CH}_2\text{O}-$ , ether groups).

OPD/MPEM (Fig. 3c, 400 MHz,  $\text{DMSO-d}_6$ ,  $\delta$  ppm): 2.50 (solvent residual peak of  $\text{DMSO}$ ), 3.24–3.70 ( $-\text{CH}_2\text{CH}_2\text{O}-$ , ether groups), 7.01–8.30 ( $-\text{HC}=\text{CH}-$ , protons on the benzene ring), 11.9–12.2 ( $-\text{NH}$ , proton in  $-\text{N}-\text{H}$  on benzimidazole ring).

### 3.2. Weight loss experimental analysis of OPD/MPEM

The variations of the weight loss for the copper specimen in 3.5 wt.%  $\text{NaCl}$  solution containing different concentrations of OPD/MPEM are shown in Fig. 4 and Table 1.

The inhibition efficiency of inhibitor,  $\text{IE}_w\%$ , for the corrosion of copper is obtained by using the following equations:

$$\theta = \frac{W}{St} \quad (1)$$

$$\text{IE}_w\% = \frac{\theta^0 - \theta}{\theta^0} \quad (2)$$

wherein  $W$  is the weight loss of the copper species,  $S$  is the total surface area of the sample,  $t$  is the immersion time,  $\theta^0$  and  $\theta$  are the corrosion rates of the copper sample without and with inhibitor, respectively.

As seen in Fig. 4 and Table 1, OPD/MPEM can produce better corrosion inhibition of copper at lower concentrations and the effect gradually increases with the increase of the concentrations of OPD/MPEM. When the dosage was  $60\text{ mg L}^{-1}$ , the corrosion inhibition efficiency got the best, which was 88.0%. This is due to the adsorption of organic molecules on copper surface, which could keep the copper surface from the corrosion caused by chloride ion and prevent the formation of cuprous chloride and oxychloride complexes. Nonetheless, when the addition amount exceeds  $60\text{ mg L}^{-1}$ , the corrosion inhibition efficiency decreases slightly with the increase of the concentration. This is because when the concentration of the corrosion inhibitor continues to increase, the dispersion of the polyether molecules themselves will result in a small amount of dispersion of the adsorption film, thereby reducing its corrosion inhibition efficiency.

### 3.3. Electrochemical polarization analysis of OPD/MPEM

The polarization curves of copper in 3.5 wt.%  $\text{NaCl}$  solution with and without different concentrations of the inhibitor OPD/MPEM were measured and the potentiodynamic polarization curves obtained from copper at 318 K are plotted in Fig. 5.

It is found that the current densities significantly decrease in the presence of different concentrations of OPD/MPEM, while the curve shapes are quite similar. This indicates that the electrochemical mechanism in the anodic and cathodic regions is not varied by the addition of the corrosion inhibitor OPD/MPEM.

As shown in Fig. 5, the corrosion potential ( $E_{\text{cor}}$ ) of the copper electrode moves in the negative direction and both the cathodic and anodic current densities decrease compared to the blank  $\text{NaCl}$  solution with the addition of corrosion inhibitor OPD/MPEM. This suggests that OPD/MPEM can effectively suppress the anodic and cathodic reaction processes simultaneously. As the suppression of the cathodic domain is more pronounced, suggesting that the influence of OPD/MPEM on the cathodic reaction is greater than that on the anodic reaction. This phenomenon could be attributed to the modification of the anodic dissolution process because the inhibitor molecules absorb on the active sites, which results in the decrease of the corrosion sites of chloride ions [11].

Table 2 shows the electrochemical parameters obtained from the Tafel plots of the copper electrode in 3.5 wt.%  $\text{NaCl}$  solution with and without different concentrations of the inhibitor OPD/MPEM at 318 K. The values of the corrosion potential ( $E_{\text{cor}}$ ), cathodic and anodic Tafel slope ( $\beta_c$ ,  $\beta_a$ ), and the corrosion current density ( $I_{\text{cor}}$ ) are calculated from Tafel extrapolation method. The inhibition efficiency ( $\text{IE}_i\%$ ) can be calculated by the following equation:

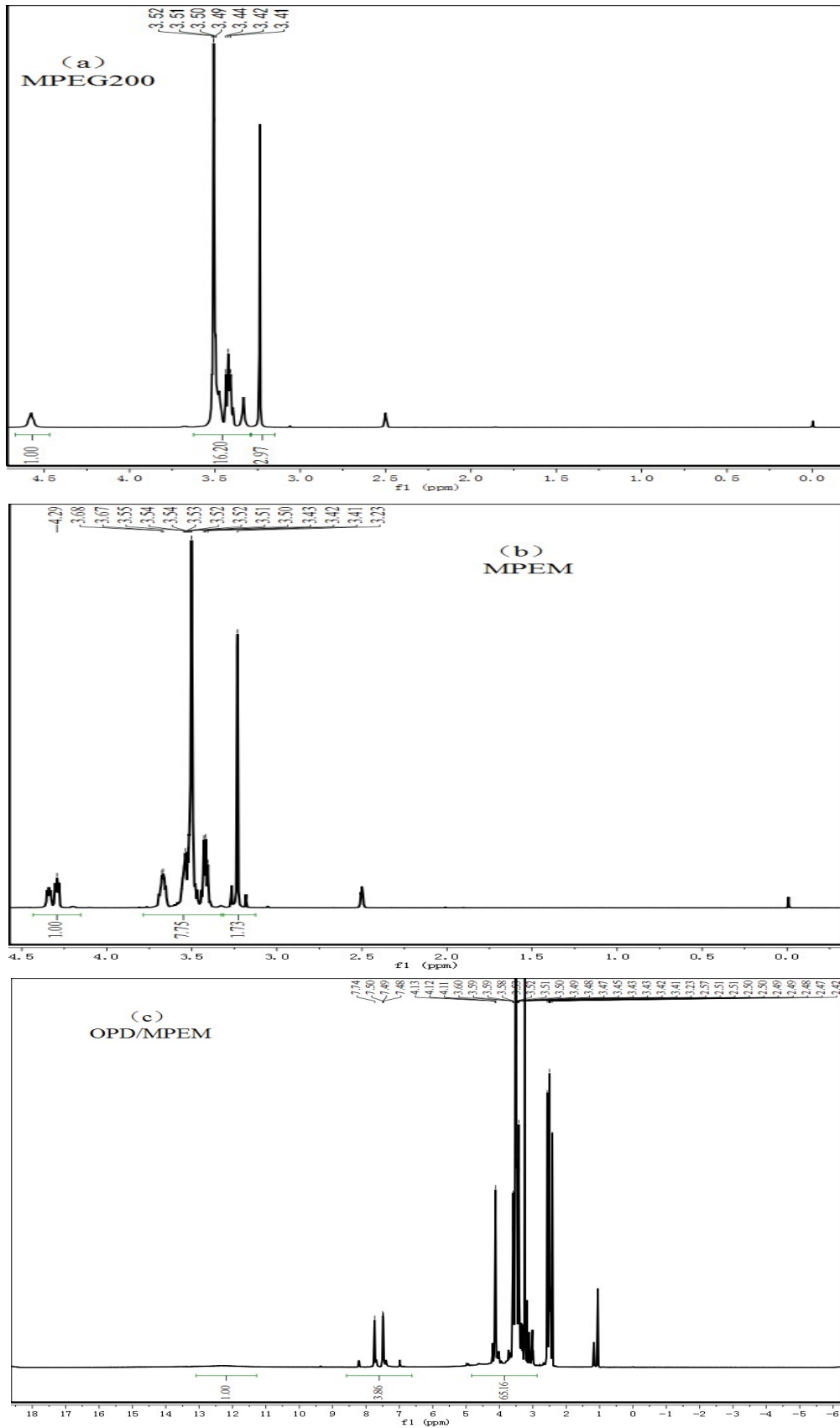


Fig. 3. The  $^1\text{H}$ -NMR spectra of MPEG (a), MPPEM (b), and OPD/MPPEM (c).

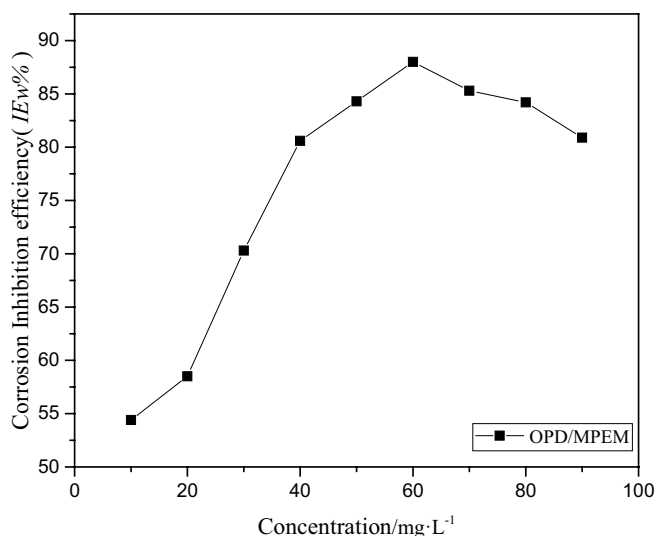


Fig. 4. Corrosion inhibition efficiency obtained from weight loss measurements for copper in 3.5 wt.% NaCl solution with various concentrations of OPD/MPPEM at 318 K for 72 h.

Table 1

Corrosion inhibition efficiency obtained from weight loss measurements for copper in 3.5 wt.% NaCl solution with various concentrations of OPD/MPPEM at 318 K for 72 h

Concentration (mg L <sup>-1</sup> )	Weight loss (g)	Corrosion rate (mm/a)	IE <sub>w</sub> (%)
0	0.1160	1.2615	–
10	0.0529	0.5753	54.4
20	0.0481	0.5231	58.5
30	0.0344	0.3741	70.3
40	0.0225	0.2447	80.6
50	0.0182	0.1979	84.3
60	0.0139	0.1512	88.0
70	0.0171	0.1860	85.3
80	0.0185	0.2012	84.2
90	0.0221	0.2403	80.9

$$IE_I \% = \frac{I_{\text{corr}}^0 - I_{\text{corr}}}{I_{\text{corr}}^0} \times 100 \quad (3)$$

wherein  $I_{\text{corr}}^0$  and  $I_{\text{corr}}$  are the corrosion current densities of copper electrode in 3.5 wt.% NaCl solutions with the presence or absence of the inhibitors, respectively.

The corrosion inhibition type of corrosion inhibitor can generally be judged according to the variation range of the corrosion potential of the electrode. It is thought that an organic inhibitor can be regarded as either anodic-type or cathodic-type if the change in  $E_{\text{corr}}$  value is above 85 mV (SEC), otherwise it is a mixed inhibitor [12]. In comparison with the copper in the blank NaCl solution,  $E_{\text{corr}}$  values in the presence of the inhibitor OPD/MPPEM slightly move to the negative direction, and the displacements are less than 85 mV (SEC), which suggests that the targeted inhibitor OPD/MPPEM plays the mixed-type inhibitor roles.

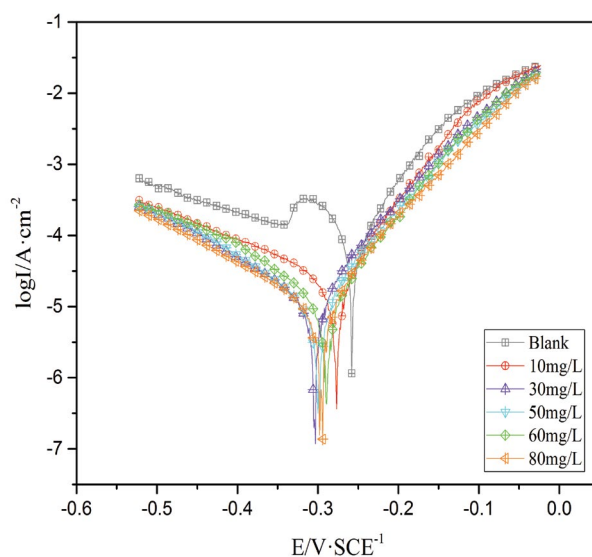


Fig. 5. Polarization curves for copper in 3.5 wt.% NaCl solution with and without different concentrations of OPD/MPPEM at 318 K.

As can be seen in Table 2, with the increase of the concentration of OPD/MPPEM from 10 to 60 mg L<sup>-1</sup> in NaCl solution,  $I_{\text{corr}}$  value reduces from 24.552 to 11.448  $\mu\text{A cm}^{-2}$ , and IE<sub>w</sub> value increases from 82.72% to 91.94%. This suggests that the film formed on the copper surface becomes denser with the increase of the concentration of OPD/MPPEM. Therefore, the copper could be effectively protected by OPD/MPPEM in the NaCl solution. On the other hand, as the concentration of OPD/MPPEM exceeds 60 mg L<sup>-1</sup>, IE<sub>w</sub> value decreases (91.62% at 80 mg L<sup>-1</sup>). This could be caused by the dispersion of the polyether molecules themselves which will give rise to a small amount of dispersion of the adsorption film. As a result, the corrosive chloride ions could easily attack the copper through the interspaces. The variations of  $\beta_c$  and  $\beta_a$  with the increase of the concentration of the target OPD/MPPEM demonstrate that the organic inhibitor film suppresses both the anodic and cathodic reactions.

#### 3.4. EIS analysis of OPD/MPPEM

EIS measurements were carried out to investigate the corrosion inhibition effect of OPD/MPPEM as well as the kinetics of the corrosion reaction process. The spectra of Nyquist, Bode, and phase angle of copper electrodes without and with various concentrations of OPD/MPPEM at the OCP immersed in 3.5 wt.% NaCl solution at 318 K for 30 min respectively are shown in Figs. 6a–c.

All the impedance plots show the typical semicircles in the high-frequency areas which are attributed to the time constant of the charge transfer and the double-layer capacitance [13]. On the other hand, the capacitive arc is not a regular semicircle. It is a result of the dispersion effect due to the change of the original electrode surface morphology caused by the rough electrode surface (surface roughness caused during the electrode grinding process) and other inhomogeneities [14]. It also shows that there is a passivation film on the surface of copper.

Table 2

Polarization parameters for copper in 3.5 wt.% NaCl solution without and with different concentrations of OPD/MPPEM at 318 K

Concentration (mg L <sup>-1</sup> )	$E_{\text{corr}}$ (V SCE <sup>-1</sup> )	$I_{\text{corr}}$ ( $\mu\text{A cm}^{-2}$ )	$\beta_c$ (mV dec <sup>-1</sup> )	$\beta_a$ (mV dec <sup>-1</sup> )	$\text{IE}_t$ (%)
0	-0.258	142.08	4.652	14.160	–
10	-0.277	24.552	4.843	14.950	82.72
30	-0.303	14.640	6.601	12.658	89.70
50	-0.298	11.876	7.174	12.990	91.64
60	-0.289	11.448	8.053	14.642	91.94
80	-0.294	11.904	6.189	12.532	91.62

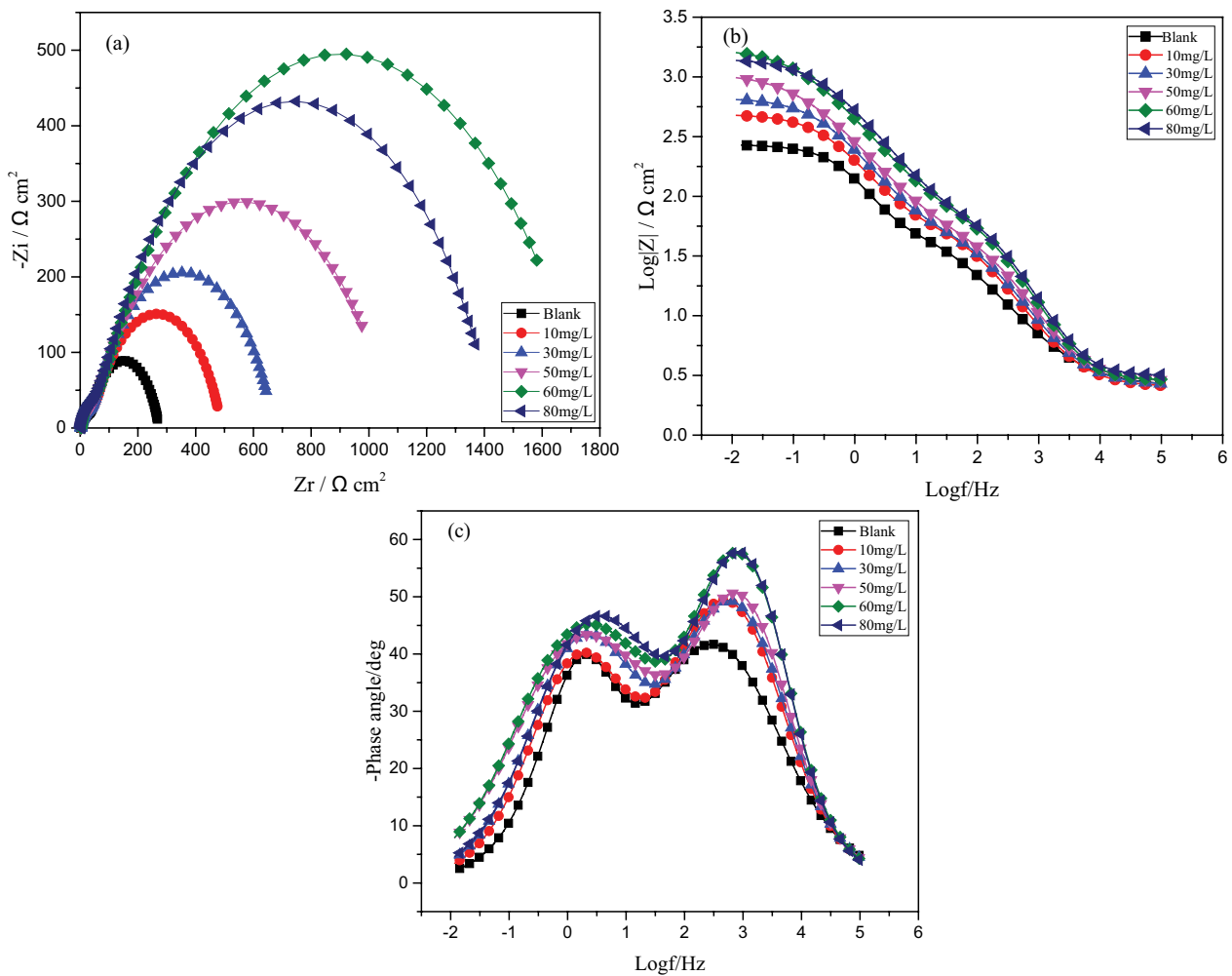


Fig. 6. Nyquist (a), Bode (b), and phase angle (c) plots for copper in 3.5 wt.% NaCl solution without and with different concentrations of OPD/MPPEM at 318 K.

For the copper electrodes covered with these corrosion inhibitor molecules, large semicircles are shown at the high-frequency area in Nyquist plots and the diameters of the semicircle gradually increase with the increase of the concentrations of OPD/MPPEM, which prove the formation of the inhibitor molecular protective film. Fig. 6a suggests that the diameter of the capacitive loop reaches the maximum at 60 mg L<sup>-1</sup> of OPD/MPPEM. On the other hand, the shapes of

the Nyquist plots for the inhibited copper electrodes are not substantially different from those of the uninhibited copper electrode, which indicates that OPD/MPPEM does not change the corrosion mechanism of copper in 3.5 wt.% NaCl solution [15].

Fig. 6b (Bode plots) shows that the impedance values over the whole frequency range greatly increase with the increase of the concentrations of OPD/MPPEM, and the

values of the impedance reach the peak as its concentration is  $60 \text{ mg L}^{-1}$ , which means the best inhibition corrosion protection is obtained [16]. On the other hand, Fig. 6c shows that the phase angle displays an enhancement with the increase of the concentrations of OPD/MPPEM, suggesting that the increase of the corrosion inhibitor molecules adsorption on the electrode surface [17]. Furthermore, the corrosion process of OPD/MPPEM possesses two relaxation time constants as can be obtained from the phase angle plots. One is dependent on the relaxation of the electrical double layer capacitor, and the other is related to the relaxation process of the adsorbed corrosion inhibitors.

Fig. 7 shows the equivalent circuit model for fitting the experimental data to analyze the electrochemical corrosion process. This model was reported to study for the copper-chloride solution interface [18], and it produces less error and the chi-square value ( $\chi^2$ ) is lower than  $1 \times 10^{-3}$ .

In this circuit,  $R_{ct}$  is the charge transfer resistance corresponding to the corrosion reaction at the copper-solution interface.  $R_s$  represents the resistance of the solution between the working and the reference electrodes.  $R_f$  is the film resistance from inhibitors and the inevitable oxide species.  $W$  is the Warburg impedance induced by the diffusion of corrosive reactants or corrosion produce species. The constant phase elements  $CPE_f$  and  $CPE_{dl}$  are used to replace the film capacitance and the double layer capacitance, respectively. The impedance of CPE ( $Z_{CPE}$ ) can be described by the following equation:

$$Z_{CPE} = Y^{-1} (i\omega)^{-n} \quad (4)$$

wherein  $Y$  is the proportional factor,  $\omega$  is the angular frequency,  $n$  is the deviation parameter, and  $i$  is the imaginary unit. The value of  $n$  ranges from  $-1$  to  $1$ , which can represent the non-uniformity of the copper surface [19]. Generally, when the value of  $n$  equals zero, the CPE represent pure resistor ( $R$ ); as for  $n = 1$ , the CPE represents pure capacitor ( $C$ ); and if  $n = -1$ , the CPE stands for inductor ( $L$ ); moreover, as  $n = 0.5$ , the CPE denotes a Warburg impedance ( $W$ ). The capacitance values of  $CPE_{dl}$  can be calculated from CPE parameter values  $Y$  and  $n$  using Eq. (5).

$$C_{dl} = \frac{Y\omega^{n-1}}{\sin\left(\frac{n\pi}{2}\right)} \quad (5)$$

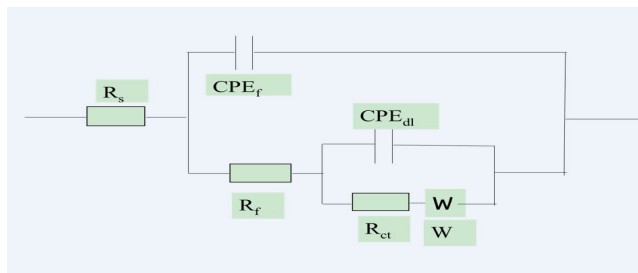


Fig. 7. The equivalent circuit model used to fit the EIS experimental data.

The addition of the inhibitor provides the lower  $Y$  values, which is the consequence of the replacement of water molecules by the corrosion inhibitor molecules at the electrode surface. Moreover,  $n$  value is apt to decrease with increase of the concentration of the corrosion inhibitors, which indicates the adsorption of organic molecules on the copper surface [20]. The thickness of the protective layer ( $d$ ) is related to  $CPE_{dl}$  according to the expression of the layer capacitance presented in Helmholtz model:

$$C_{dl} = \frac{\varepsilon^0 \varepsilon}{d} A \quad (6)$$

wherein  $d$  is the thickness of the film,  $A$  is the surface area of the electrode,  $\varepsilon^0$  is the permittivity of the air, and  $\varepsilon$  is the local dielectric constant. The  $\varepsilon^0$  and  $A$  are the constant elements for a definite system so that Equation 6 suggests that  $C_{dl}$  in the inhibitor systems could be lowered by the increase of the adsorption film area, the decrease in the local dielectric constant, and/or the increase in the thickness of the protective layer. Furthermore, the more inhibitors adsorbed on the copper surface, the greater the thickness of the protective layer and the better the protective effect of copper.

The polarization resistance  $R_p$  is expressed by Eq. (7):

$$R_p = R_{ct} + R_f \quad (7)$$

The inhibition efficiency ( $IE_p$  %) can be calculated from the  $R_{ct}$  values by the following equation:

$$IE_p \% = \frac{R_{ct} - R_{ct}^0}{R_{ct}} \times 100 \quad (8)$$

wherein  $R_{ct}$  and  $R_{ct}^0$  are the charge-transfer resistances in uninhibited and inhibited solutions, respectively.

The corresponding impedance parameters for  $R(Q(R(Q(RW))))$  are given in Table 3. As can be seen from Table 3,  $C_f$  values decrease until the optimal concentration appears, which is due to the ionic conductivity of the surface film that decreases with the increase of the concentration of the inhibitors.  $C_{dl}$  values decrease with the increase of the concentration of OPD/MPPEM until the concentration reach  $60 \text{ mg L}^{-1}$ . This is because of the gradual replacement of water molecules by the adsorption of corrosion inhibitor molecules at the copper electrode surface, resulting in the production of a protective film on the copper surface that prevents the mass and charge transfers.

Table 3 also reveals that  $R_{ct}$  increases with the enhancement of the concentration of OPD/MPPEM, suggesting that the protecting film on the copper electrode surface is formed and the charge transfer process is impeded as the uncovered area for this process is diminished due to the adsorption of more corrosion inhibitor molecules at the copper/electrolyte interface.

### 3.5. Adsorption isothermal analysis of OPD/MPPEM

It is well known that organic compounds generally form an adsorption film by adsorbing on metal surfaces to protect metals from corrosive environments. Therefore, it is very

Table 3

Electrochemical parameters calculated from EIS measurements for copper in 3.5 wt.% NaCl solution with different concentrations of OPD/MPPEM at 318 K

$C/\text{mg L}^{-1}$	$R_s$	$R_f$	$R_{ct}$	CPE <sub>f</sub>		CPE <sub>dl</sub>		W	IE <sub>p</sub> %
				$C_f$	$n_1$	$C_{dl}$	$n_2$		
0	2.572	60.19	210.5	173.23	0.6621	180.25	0.8954	0.7393	–
10	2.526	61.8	424.3	73.54	0.7636	120.42	0.7611	743000	50.4
30	2.625	55.11	612.3	54.32	0.7791	98.77	0.7298	1.019	65.6
50	2.810	49.44	1033	43.65	0.8164	69.76	0.6497	138500	79.6
60	2.878	69.41	1684	30.21	0.8711	29.94	0.6588	63.02	87.5
80	3.134	69.45	1363	39.87	0.8838	45.43	0.6977	3395	84.6

important to study the adsorption mechanism of corrosion inhibitor molecules on the metal surface. The adsorption mechanism of the corrosion inhibitor molecule at the metal-solution interface can be studied and predicted by means of adsorption thermodynamics, and the adsorption type on the metal surface can be judged accordingly.

Adsorption isotherms are an important way to study the adsorptive properties of corrosion inhibitor molecules to provide information about the nature of corrosion inhibitor and metal surface interactions. In this paper, adsorption isotherms of OPD/MPPEM on the copper surface were investigated by means of adsorption isotherms such as Flory–Huggins, Dhar–Flory–Huggins, Bockris–Swinkels, Freundlich, and Langmuir.

The results show that Langmuir adsorption isotherm can best explain the adsorption behavior of OPD/MPPEM on the copper surface in 3.5 wt.% NaCl solution.

The degrees of surface coverage ( $\theta$ ) for different concentrations of the inhibitors in 3.5 wt.% NaCl solution can be calculated by the electrochemical polarization measurement by using the following equation:

$$\theta = \frac{\theta^0 - \theta}{\theta^0} \quad (9)$$

And then, the expression of Langmuir isotherm can be showed as the following equation:

$$\frac{C_{inh}}{\theta} = C_{inh} + \frac{1}{K_{ads}} \quad (10)$$

wherein  $\theta^0$  and  $\theta$  are the corrosion rates of the copper sample without and with inhibitor, respectively,  $K_{ads}$  is the equilibrium constant of the inhibitor adsorption process,  $C_{inh}$  is the inhibitor concentration. Fig. 8 shows the Langmuir adsorption isotherm curve of OPD/MPPEM in 3.5 wt.% NaCl solution at 318 K.

As can be seen from Fig. 8,  $C_{inh}/\theta$  and  $C_{inh}$  show a typical linear relationship, and its linear fitting coefficient ( $R^2$ ) is 0.99989, which proves that the adsorption of OPD/MPPEM inhibitor molecules on the copper surface can be well performed using the Langmuir adsorption isotherm curve model. According to the adsorption characteristics of the corrosion inhibitor, the nature of the corrosion inhibitor can be deduced. In the aqueous solution, the metal surface is always covered by the adsorbed water molecules, and the

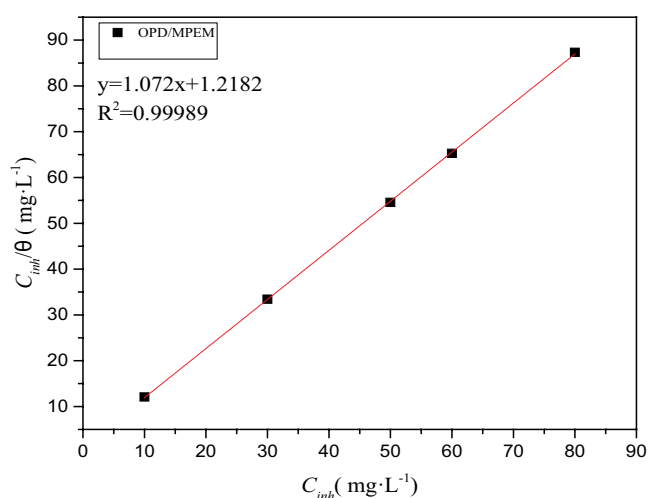


Fig. 8. Langmuir adsorption plots for copper in 3.5 wt.% NaCl solution at 318 K in various concentrations of OPD/MPPEM.

adsorption of the corrosion inhibitor on the copper surface is considered as an alternative adsorption process between the corrosion inhibitor molecules in the water phase and the water molecules adsorbed on the copper surface. According to the Langmuir isotherm adsorption theory, a corrosion inhibitor molecule replaces water molecules on the metal surface during the adsorption process, and then the equilibrium constant  $K_{ads}$  can be calculated by the following equation:

$$K_{ads}^0 = \frac{1}{55.5} \exp\left(-\frac{\Delta G_{ads}^0}{RT}\right) \quad (11)$$

thus

$$\Delta G_{ads}^0 = -RT(\ln 55.5 K_{ads}^0) \quad (12)$$

wherein  $R$  is the molar gas constant (8.314 J mol<sup>-1</sup> K<sup>-1</sup>),  $T$  is the thermodynamic temperature of the experiment, and the value 55.5 is the molar concentration of water in solution with units of kilojoules per mole. In general, when  $\Delta G_{ads}^0$  is negative, it indicates that the adsorption of inhibitor molecules on the metal surface is spontaneous, and the interaction of the inhibitor molecules with the metal surface is also

strong. Under normal circumstances, when  $\Delta G^{\circ}_{\text{ads}}$  is less than  $-40 \text{ KJ mol}^{-1}$ , it indicates that organic molecules share or transfer their electrons to the metal surface and form coordination bonds such as chemical adsorption. When  $\Delta G^{\circ}_{\text{ads}}$  is greater than  $-20 \text{ KJ mol}^{-1}$ , there is electrostatic interaction between organic molecules and metal surface atoms, belonging to physical adsorption. When the value of  $\Delta G^{\circ}_{\text{ads}}$  is in the range of  $-20 \text{ KJ mol}^{-1}$  to  $-40 \text{ KJ mol}^{-1}$ , the adsorption of organic molecules on the metal surface includes both physical adsorption and chemical adsorption [21].

From Fig. 8 it can be concluded that  $K_{\text{ads}} = 3.05 \times 10^5 \text{ L mol}^{-1}$ , so that from Eq. (12), it is possible to calculate  $\Delta G^{\circ}_{\text{ads}} = -44.01 \text{ KJ mol}^{-1}$ . The result shows that the adsorption behavior of OPD/MPPEM on the copper surface was mainly controlled by chemical adsorption behavior in 3.5 wt.% NaCl solution.

### 3.6. SEM and energy-dispersive spectrometer (EDS) analysis of OPD/MPPEM

The surface morphology of copper sample immersed in 3.5 wt.% NaCl solution at 318 K for 72 h in the absence and in the presence of  $60 \text{ mg L}^{-1}$  of OPD/MPPEM was studied by SEM. Fig. 9 shows the surface morphology of copper

specimens (a) before, (b) after being immersed in 3.5 wt.% solution, (c) after being immersed in the corrosive solution of OPD/MPPEM, and (d) after the removal (by pickling) of the inhibiting film.

From Fig. 9a it can be seen that the un-corroded copper coupons have a very smooth surface and can clearly see the metal texture of the surface. Fig. 9b shows that the copper coupons have not been added with OPD/MPPEM in 3.5 wt.% NaCl solution, the result showed that the test piece was seriously corroded, which the surface was uneven and there were various kinds of corrosion pits with different depths. Fig. 9c shows the surface morphology of unpickled copper after a 72 h weight loss test ( $T = 318 \text{ K}$ ) in  $60 \text{ mg L}^{-1}$  OPD/MPPEM corrosion inhibitor solution. Its surface is flat compared to (b), and a layer of more obvious adsorption film can be seen, which shows that it forms an adsorption film on the surface of the copper after adding the inhibitor OPD/MPPEM, thereby slowing down the copper corrosion in the 3.5 wt.% NaCl solution. Fig. 9d shows the surface morphology of the acid-washed copper after a 72 h weight loss test ( $T = 318 \text{ K}$ ) in a solution containing  $60 \text{ mg/L}$  OPD/MPPEM corrosion inhibitor. It can be seen that the copper coupons are generally flat after desorption film, although

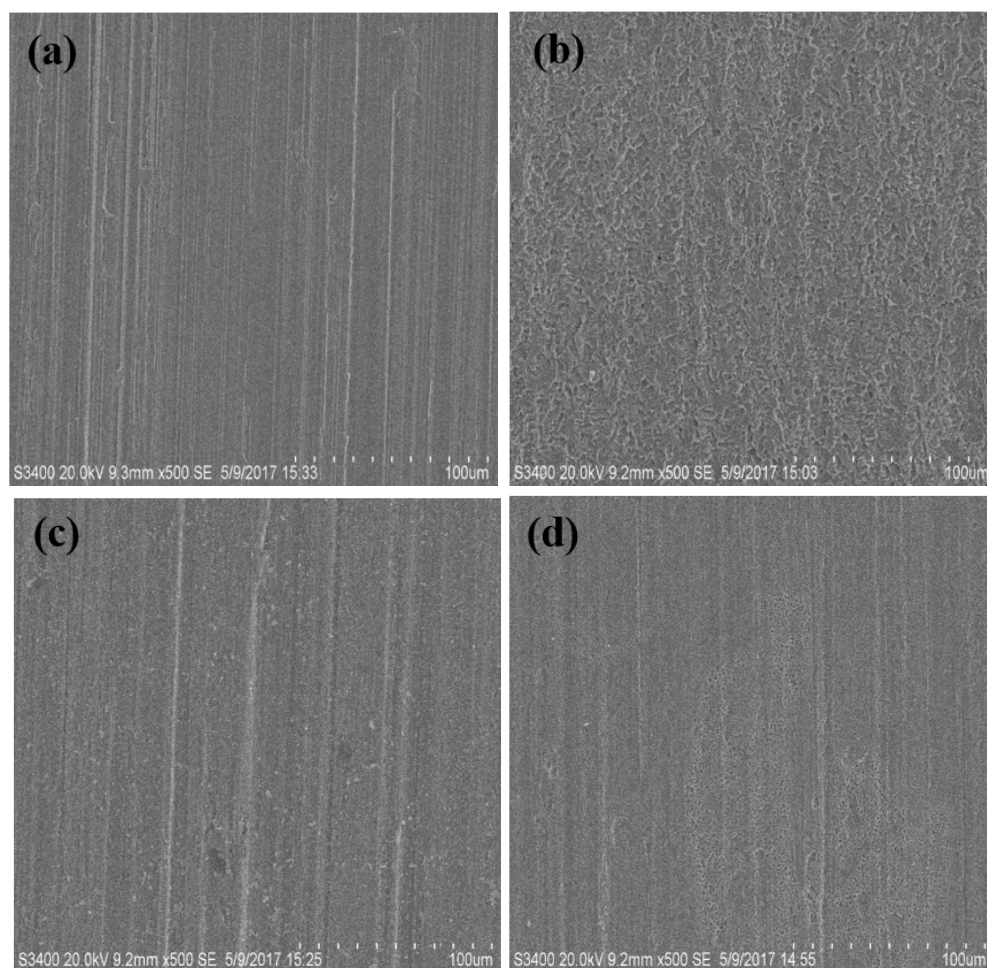


Fig. 9. SEM micrographs of the surface of Cu, (a) before and after being immersed for 72 h in 3.5 wt.% NaCl solutions: (b) without inhibitor, (c) with  $60 \text{ mg L}^{-1}$  of OPD/MPPEM, and (d) after the removal of the inhibiting film.

there were some small corrosion pits on the surface. This indicates that the copper coupons are protected and can significantly reduce the corrosion of the copper after adding OPD/MPPEM.

Fig. 10 presents the results of energy-dispersive spectrometer (EDS) analysis. The copper, carbon, oxygen, chloride and sodium are determined after the immersion in the solution during 72 h. The content of each element on copper surface obtained from EDS after the immersion in 3.5 wt.% NaCl solutions without and with inhibitors for 72 h at 318 K is shown in Table 4. The results show that the composition of the detected elements on the copper surface which was immersed in 3.5 wt.% NaCl solution containing 60 mg L<sup>-1</sup> OPD/MPPEM for 72 h included 23.15% C, 7.15% O, 6.32% Na, 3.62% Cl and 59.76% Cu, respectively. This indicates that the organic inhibitor molecules are strongly adsorbed on the copper forming the Cu-OPD/MPPEM bond to prevent corrosion.

### 3.7. Quantum chemical calculations

The optimized geometry and frontier molecular orbital density distributions of OPD/MPPEM are presented in Fig. 11. Fig. 11a shows the molecular structure of corrosion inhibitor after geometric optimization, (b) is the HOMO electron density of the OPD/MPPEM inhibitor molecule while (c) is the LUMO electron density.

As can be seen, the HOMO electron density of the OPD/MPPEM inhibitor molecules is mainly distributed on the long polyether chains, while the LUMO electron density is mainly distributed on the benzimidazole ring. This suggests that the electrons on the polyether chain are preferentially adsorbed on the copper surface in the inhibitor molecular structure, and the electrons of the corrosion inhibitor and the empty d-orbital of the copper surface form a special covalent bond (coordination bond). The feedback bond can also be formed by accepting electrons from the copper surface through the antibonding orbitals on the benzimidazole ring. In this way, OPD/MPPEM molecules interact with the surface of copper, so that the corrosion inhibitor molecules form a denser and more stable corrosion inhibitor molecular protective film on the surface of the copper, blocking the electricity generated

Table 4

Contents of the elements on the copper surface obtained from EDS after immersion in 3.5 wt.% NaCl solutions without and with OPD/MPPEM at 318 K

Element	Blank	OPD/MPPEM
C (wt.%)	0	23.15
O (wt.%)	0	7.15
Na (wt.%)	0	6.32
Cl (wt.%)	0	3.62
Cu (wt.%)	100	59.76

on the copper surface and corrosive substances in the solution, thereby forming a good protective effect on the copper.

According to Koopman's theorem, the values of  $E_{\text{HOMO}}$  and  $E_{\text{LUMO}}$  of the inhibitor molecule are associated with the ionization potential ( $I$ ) and the electron affinity ( $A$ ), respectively. The ionization potential and the electron affinity are defined as  $-E_{\text{HOMO}}$  and  $-E_{\text{LUMO}}$ , respectively. The obtained values of the ionization potential ( $I$ ) and the electron affinity ( $A$ ) are used to calculate the electronegativity ( $\chi$ ) and the global hardness ( $\eta$ ).

The fraction of electrons transferred from the inhibitor molecules to the metallic atom ( $\Delta N$ ) is calculated according to Pearson's theory, as shown in the following equation:

$$\Delta N = \frac{\chi_{\text{Cu}} - \chi_{\text{inh}}}{2(\eta_{\text{Cu}} + \eta_{\text{inh}})} \quad (13)$$

wherein the theoretical value for the electronegativity of bulk copper,  $\chi_{\text{Cu}} = 4.48$  eV, is used, and a global hardness of  $\eta_{\text{Cu}} = 0$  was used. And the electronegativity ( $\chi_{\text{inh}}$ ) and the global hardness ( $\eta_{\text{inh}}$ ) of the inhibitor molecule are approximated as Eqs. (14) and (15), respectively. During the interaction between the inhibitor molecule and the copper surface, when  $\Delta N > 0$ , electrons flow from the inhibitor molecule to the copper surface. On the other hand, if  $\Delta N < 0$ , the electron transfer direction will be reversed. Also, if the value of  $\Delta N$  is lower than 3.6, the inhibition rate of the corrosion

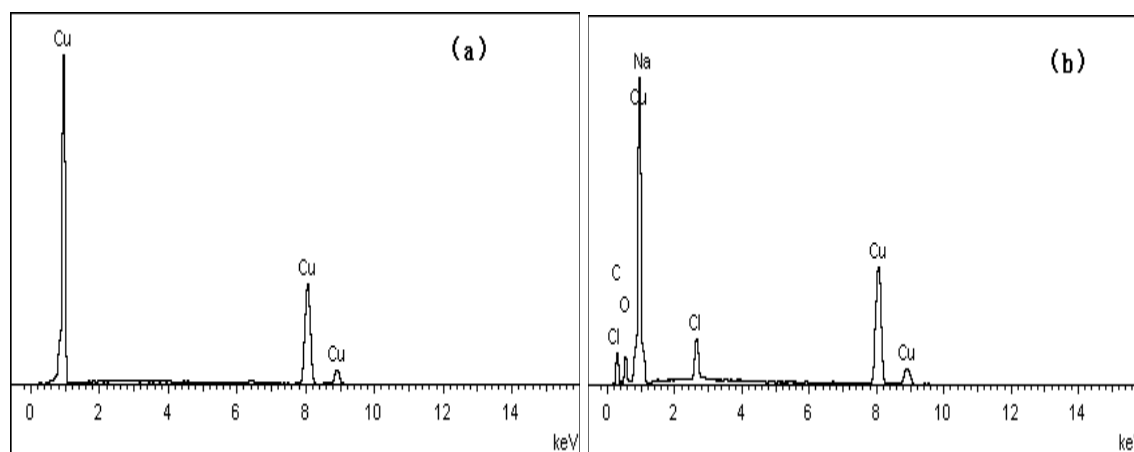


Fig. 10. EDS analysis of the copper surface presented in (a) Fig. 9a and (b) Fig. 9d.

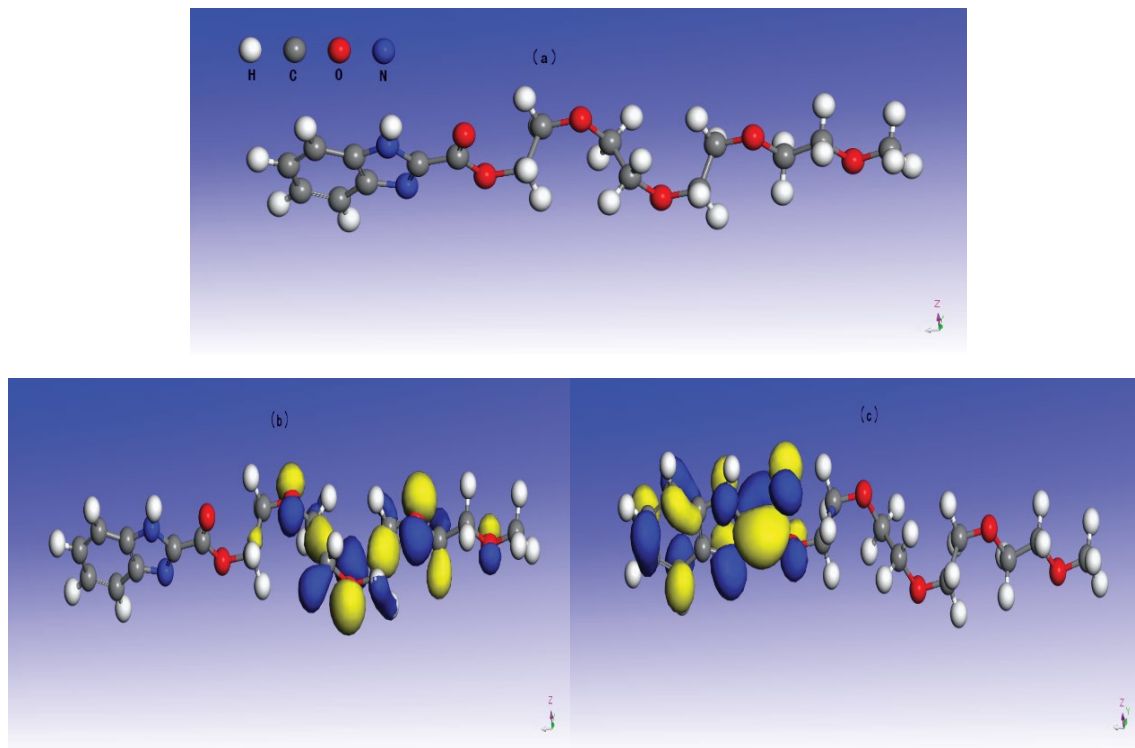


Fig. 11. Optimized geometry and frontier molecular orbital density distributions of OPD/MPEM.

inhibitor molecules will increase as the metal electron supply capability increases.

$$\chi = \frac{I + A}{2} \quad (14)$$

$$\eta = \frac{I - A}{2} \quad (15)$$

From the parameters in Table 5, it can be seen that the inhibitor molecule OPD/MPEM has higher reactivity (lower  $\Delta E$ ).  $\chi_{\text{inh}}$  (3.841 eV) <  $\chi_{\text{Cu}}$  (4.48 eV),  $0 < \Delta N < 3.6$ , so the corrosion inhibitor can impart electrons to the copper surface by forming a coordination bond, thereby forming a protective film to delay copper corrosion.

Table 5  
Quantum chemical parameters calculated using the DMol3 with the GGA/BLYP functional and DND basis set for OPD/MPEM model

Inhibitor	OPD/MPEM
$E_{\text{HOMO}}$ (eV)	-5.385
$E_{\text{LUMO}}$ (eV)	-2.296
$\Delta E$ (eV)	3.089
$\chi$ (eV)	3.841
$\eta$ (eV)	1.545
$\Delta N$	0.207

#### 4. Conclusions

This study presents a new benzotriazole derivative containing a polyether chain as the corrosion inhibitor for copper in 3.5 wt.% NaCl solution based on rational molecular preconstruction. The corrosion inhibition efficiencies determined by the weight loss, the polarization curves and EIS experiments respectively show that the inhibitor OPD/MPEM exhibits the best corrosion inhibition efficiency approximately 88.0% at 60 mg L<sup>-1</sup>. The electrochemical determination indicates that OPD/MPEM acts as a mixed-type corrosion inhibitor, which displays inhibition in the anodic and cathodic processes of the corrosion reactions through the formation of a protective layer on the copper surface and the adsorbed layer over the copper surface could be seen by SEM analysis. The adsorption of the inhibitor on copper is found to follow Langmuir isotherm, and the inhibitor shows the adsorption of the chemical phenomena on the copper surface based on analysis of the value of  $\Delta G^{\circ}_{\text{ads}}$  obtained. The quantum chemical calculation shows that the OPD/MPEM molecule has high reactivity and strong interaction on the copper surface, which denotes the high corrosion inhibition efficiency of OPD/MPEM owned. The results presented herein greatly guide us to prepare neat corrosion inhibitors for copper in a sodium chloride medium.

#### Acknowledgments

This work was supported by the research fund for young teachers of Chengxian College of Southeast University (Z0016), the National Nature Science Foundation of China (51673040), the Prospective Joint Research Project of Jiangsu

Province (BY2016076-01), Scientific Innovation Research Foundation of College Graduate in Jiangsu Province (KYLX16\_0266), and a Project Funded by the Priority Academic Program Development of Jiangsu Higher Education Institutions (PAPD) (1107047002). The Fundamental Research Funds for the Central Universities (2242018k30008), Fund Project for Transformation of Scientific and Technological Achievements of Jiangsu Province of China (BA2016105), Based on scientific research SRTP of southeast University (T16192020), and the Scientific Research Foundation of Graduate School of Southeast University (YBJJ1417).

## References

- [1] D.Q. Zhang, X.M. He, Q.R. Cai, L.X. Gao, G.S. Kim, pH and iodide ion effect on corrosion inhibition of histidine self-assembled monolayer on copper, *Thin Solid Films*, 518 (2010) 2745–2749.
- [2] H.M. Ezuber, A.W. Al Shater, A. Badawy, Influence environmental of parameters on the corrosion behavior of 90/10 cupronickel tubes in 3.5% NaCl, *Desal. Wat. Treat.*, 57 (2016) 6670–6679.
- [3] J.A. Carew, M. Abdeljawad, Y. Alwazzan, Evaluation of corrosion-resistant alloys for desalination applications, *Desalination* 95 (1994) 53–74.
- [4] A. Moreau, Study of the oxidation-reduction mechanism of copper in hydrochloric-acid solutions. 2. The Cu-CuCl-CuCl<sub>2</sub>(-) and Cu-Cu<sub>2</sub>(OH)<sub>3</sub>Cl+Cu<sup>2+</sup> systems, *Electrochim. Acta*, 26 (1981) 1609–1616.
- [5] A. Al-Hashem, J. Carew, The use of electrochemical impedance spectroscopy to study the effect of chlorine and ammonia residuals on the corrosion of copper-based and nickel-based alloys in seawater, *Desalination*, 150 (2002) 255–262.
- [6] C. Deslouis, O.R. Mattos, M.M. Musiani, B. Tribollet, Comments on mechanisms of copper electrodisolution in chloride media, *Electrochim. Acta*, 38 (1993) 2781–2783.
- [7] S.L. da Costa, S.M. Agostinho, K. Nobe, Rotating ring-disk, electrode studies of Cu-Zn alloy electrodisolution in 1M HCl: effect of benzotriazole, *J. Electrochem. Soc.*, 140 (1993) 3483–3488.
- [8] A. Atta, G. El-Mahdy, H. Al-Lohedan, Preparation and application of crosslinked poly(sodium acrylate)-coated magnetite nanoparticles as corrosion inhibitors for carbon steel alloy, *Molecules*, 20 (2015) 1244–1261.
- [9] H. Wilson, Near-infrared Fourier transform surface enhanced Raman scattering detection of mercaptobenzothiazole on smooth copper, *Vib. Spectrosc.*, 7 (1994) 287–291.
- [10] A.R. Katritzky, X. Lan, J.Z. Yang, O.V. Denisko, Properties and synthetic utility of N-substituted benzotriazoles, *Chem. Rev.*, 98 (1998) 409–548.
- [11] T.T. Qin, J. Li, H.Q. Luo, M. Li, N.B. Li, Corrosion inhibition of copper by 2,5-dimercapto-1,3,4-triazazole monolayer in acidic solution, *Corros. Sci.*, 53 (2011) 1072–1078.
- [12] A. Satapathy, K.G. Gunasekaran, S.C. Sahoo, Corrosion inhibition by justicia gendarussa plant extra in hydrochloric acid solution, *Corros. Sci.*, 51 (2009) 2848–2856.
- [13] Z. Tao, S. Zhang, W. Li, Corrosion inhibition of mild steel in acidic solution by some oxo-triazole derivatives, *Corros. Sci.*, 51 (2009) 2588–2595.
- [14] M. Hosseini, M. Sfi, M. Ghorbani, Asymmetrical Schiff bases as inhibitors of mild steel corrosion in sulphuric acid media, *Mater. Chem. Phys.*, 78 (2003) 800–808.
- [15] E.M. Sherif, S.M. Park, Inhibition of copper corrosion in 3.0% NaCl solution by N-phenyl-1,4-phenylenediamine, *J. Electrochem. Soc.*, 152 (2005) B428–B433.
- [16] S.V. Lamaka, M.L. Zheludkevich, K.A. Yasakau, R. Serra, S.K. Poznyak, M.G.S. Ferreira, Nanoporous titania interlayer as reservoir of corrosion inhibitors for coatings with self-healing ability, *Prog. Org. Coat.*, 58 (2007) 127–135.
- [17] S.M. Sherif, R.M. Erasmus, J.D. Comins, Inhibition of copper corrosion in acidic chloride pickling solutions by 5-(3-aminophenyl)-tetrazole as a corrosion inhibitor, *Corros. Sci.*, 50 (2008) 3439–3445.
- [18] S. Hong, W. Chen, H.Q. Luo, Inhibition effect of 4-aminoantipyrine on the corrosion of copper in 3 wt.% NaCl solution, *Corros. Sci.*, 57 (2012) 270–278.
- [19] D.K. Yadav, M.A. Quraishi, B. Maiti, Inhibition effect of some benzylidenes on mild steel in 1 M HCl: an experimental and theoretical correlation, *Corros. Sci.*, 55 (2012) 254–266.
- [20] W. Li, Q. He, C.L. Pei, B.R. Hou, Experimental and theoretical investigation of the adsorption behaviour of new triazole derivatives as inhibitors for mild steel corrosion in acid media, *Electrochim. Acta*, 52 (2007) 6386–6394.
- [21] K.G. Zhang, W.Z. Yang, X.S. Yin, Y. Chen, Y. Liu, J.X. Le, B. Xu, Amino acids modified konjac glucomannan as green corrosion inhibitors for mild steel in HCl solution, *Carbohydr. Polym.*, 181 (2018) 191–199.